Novel Furosemide Cocrystals and Selection of High Solubility Drug Forms

N. RAJESH GOUD,[1] SWARUPA GANGAVARAM,[2] KUTHURU SURESH,[1] SHARMISTHA PAL,[3] SULUR G. MANJUNATHA,[3] SUDHIR NAMBIAR,[3] ASHWINI NANGIA[1,2]

[1]School of Chemistry, University of Hyderabad, Prof. C.R. Rao Road, Central University PO, Gachibowli, Hyderabad 500 046, India

[2]Technology Business Incubator, University of Hyderabad, Prof. C. R. Rao Road, Central University PO, Gachibowli, Hyderabad 500 046, India

[3]Pharmaceutical Development, AstraZeneca India Pvt. Ltd., Bellary Road, Hebbal, Bangalore 560 024, India

Received 21 July 2011; revised 24 September 2011; accepted 13 October 2011

Published online 11 November 2011 in Wiley Online Library (wileyonlinelibrary.com). DOI 10.1002/jps.22805

ABSTRACT: Furosemide was screened in cocrystallization experiments with pharmaceutically acceptable coformer molecules to discover cocrystals of improved physicochemical properties, that is high solubility and good stability. Eight novel equimolar cocrystals of furosemide were obtained by liquid-assisted grinding with (i) caffeine, (ii) urea, (iii) *p*-aminobenzoic acid, (iv) acetamide, (v) nicotinamide, (vi) isonicotinamide, (vii) adenine, and (viii) cytosine. The product crystalline phases were characterized by powder x-ray diffraction, differential scanning calorimetry, infrared, Raman, near IR, and ^{13}C solid-state NMR spectroscopy. Furosemide–caffeine was characterized as a neutral cocrystal and furosemide–cytosine an ionic salt by single crystal x-ray diffraction. The stability of furosemide–caffeine, furosemide–adenine, and furosemide–cytosine was comparable to the reference drug in 10% ethanol–water slurry; there was no evidence of dissociation of the cocrystal to furosemide for up to 48 h. The other five cocrystals transformed to furosemide within 24 h. The solubility order for the stable forms is furosemide–cytosine > furosemide–adenine > furosemide–caffeine, and their solubilities are approximately 11-, 7-, and 6-fold higher than furosemide. The dissolution rates of furosemide cocrystals were about two times faster than the pure drug. Three novel furosemide compounds of higher solubility and good phase stability were identified in a solid form screen. © 2011 Wiley Periodicals, Inc. and the American Pharmacists Association J Pharm Sci 101:664–680, 2012
Keywords: bioavailability; co-crystal; crystallography; dissolution; furosemide; solid dosage form; solubility; stability; thermal analysis; x-ray diffractometry

INTRODUCTION

Poor aqueous solubility is a major bottleneck in the development of new drug molecules as pharmaceutical formulations.[1] More than 80% of marketed drugs are sold as tablets; 40% drugs in the marketplace have poor solubility and, more alarmingly, almost 80–90% of drug molecules that are at advanced stages of drug development will pose a solubility problem.[2] Drugs are classified into four categories in the Biopharmaceutics Classification System[3,4] (BCS): class I (high solubility, high permeability), class II (low solubility, high permeability), class III (high solubility, low permeability), and class IV (low solubility, low permeability). Low solubility drugs are those with a concentration of <20 mg/L in water. A well-accepted parameter for solubility is the dimensionless quantity D_0, or dose number. D_0 is the ratio of the highest drug dose strength in the administered volume (taken as 250 mL = a glass of water) to the saturation solubility of that drug in water (measured in mg/L). $D_0 < 1$ for high solubility drugs and D_0 is 25 to 100 for low solubility drugs. This value can go as high as 1000 or even 10,000. In addition to good oral absorption, permeability in the gastrointestinal tract is equally

Additional Supporting Information may be found in the online version of this article. Supporting Information

Correspondence to: A. Nangia (Telephone: +91-40-23134854; Fax: +91-40-23012460; E-mail: ashwini.nangia@gmail.com); Sharmistha Pal (Telephone: +91-80-66213000; Fax: +91-80-23621214; E-mail: sharmistha.pal@astrazeneca.com)

Journal of Pharmaceutical Sciences, Vol. 101, 664–680 (2012)

important so that the drug can bind to the receptor target. The reference standard for defining high or low permeability boundary is the *n*-octanol/water partition coefficient for metoprolol, which has log $P_{ow} = 1.72$.

Furosemide (Lasix) is a loop diuretic drug commonly used in the treatment of hypertension and edema. It is a BCS class IV drug,[5,6] that is of low solubility (6 mg/L in water) and low permeability (log P_{ow} 1.4). The highest dose strength of furosemide is 80 mg, which means that it has a D_0 number of 53. The practiced approaches to improve the solubility of furosemide may be classified into two broad categories: (1) altering the physicochemical property of the drug substance and (2) improving the way in which the drug is processed or formulated. The cocrystals strategy described in this work is currently a popular approach to modify the physicochemical properties of drugs.[7,8] A closely related method for solid form modification is that of fast dissolving furosemide polymorphs,[9–13] which were first characterized more than 20 years ago. The stabilization of nanoparticles[14] and amorphous phases[15] to achieve high dissolution rates by particle size reduction, cogrinding, and coprecipitation of the drug with crospovidone,[16] solid dispersions with polymers,[17] complexation with β cyclodextrins,[18–20] calix[n]arenes,[21] emulsification,[22] micelle formation,[23] SEDDS (self-emulsifying drug delivery systems),[24] micronization and spray drying,[25] etc. have also been reported for furosemide.

The use of pharmaceutical cocrystals has gained increasing popularity in the past decade[26–28] as a supramolecular approach to improve the physicochemical and pharmacokinetic behavior of drug substances. Furosemide has three functional groups for hydrogen bonding to make cocrystals: COOH, SO_2NH_2, and NH. Of these, the carboxylic acid and sulfonamide functional groups are well studied and known to give robust supramolecular synthons[29,30] via O—H···O and N—H···O hydrogen bonds in cocrystals. Our objective was to use COOH and SO_2NH_2 functional groups in heterosynthons with complementary coformer molecules, such as pyridine,[31] $CONH_2$,[32] NH_2,[33] and pyridine-N-oxide[34], etc. with the idea that a multicomponent crystalline adduct will be produced by self-assembly in the solid state. Within the domain of solid form modification strategies, we noted that apart from the metastable polymorphs of furosemide with higher dissolution rates,[9,10] a crystal engineering approach to tune the physicochemical characteristics of furosemide has not been reported in the literature. Furosemide salts with amino acids and their solubility characteristics were reported in a U.S. patent 5182300.[35] Furosemide is relatively stable to photodegradation in alkaline medium, but the molecule rapidly degrades in acidic conditions.[36] Even though there was good success in achieving faster dissolution rates with furosemide polymorphs, observations such as the transformation of these metastable forms to the stable modification during dissolution experiments or on storage made these results less attractive for further drug development. The fact remains that furosemide is still marketed in its stable crystalline modification (Form 1)[13] despite its poor aqueous solubility. In this background, we carried out a study on pharmaceutical cocrystals[37,38] of furosemide with the idea that being crystalline in nature they are relatively more stable and less prone to accidental phase transformations. A pharmaceutical cocrystal is defined as a stoichiometric hydrogen-bonded complex in the solid state between the active drug species and a suitable coformer molecule that is safe for human consumption (selected from the *generally recognized as safe* (GRAS) list[39] of U.S. *Food and Drug Administration*).

RESULTS AND DISCUSSION

Furosemide was cocrystallized with several coformers containing CONH and COOH functional groups with the intent of making cocrystals. The coformer selection was kept as broad as possible to widen the possibility for functional group pairing through hydrogen bonds. Non-GRAS molecules were excluded because our end goal was to make cocrystals for pharmaceutical form development. Thus even though pyridine-N-oxides are known to form strong and reliable heterosynthons with the sulfonamide group,[34] they were excluded because there is no pyridine-N-oxide compound of the GRAS status.[39] We obtained the following new crystalline phases (Scheme 1) in solution crystallization, manual grinding, and slurry crystallization screen for novel furosemide cocrystals: (i) furosemide –caffeine (FUROS–CAF), (ii) furosemide –urea (FUROS–UREA), (iii) furosemide-*p*-aminobenzoic acid (FUROS–PABA), (iv) furosemide –acetamide (FUROS–ACT), (v) furosemide –nicotinamide (FUROS–NIC), (vi) furosemide –isonicotinamide (FUROS–INIC), (vii) furosemide –adenine (FUROS–ADEN), and (viii) furosemide –cytosine (FUROS–CYT). The solvents used for cocrystallization are given in the Experimental section. A complete list of all coformers attempted with furosemide under different cocrystallization conditions is given in the Supporting Information (Table S1).

Characterization of Cocrystals

All the above-mentioned crystalline phases were characterized by powder x-ray diffraction (PXRD), infrared, near infrared and Raman spectroscopy (IR, NIR, Raman), solid-state NMR spectroscopy (ss-NMR), and differential scanning calorimetry (DSC) techniques. Microcrystalline powders were obtained

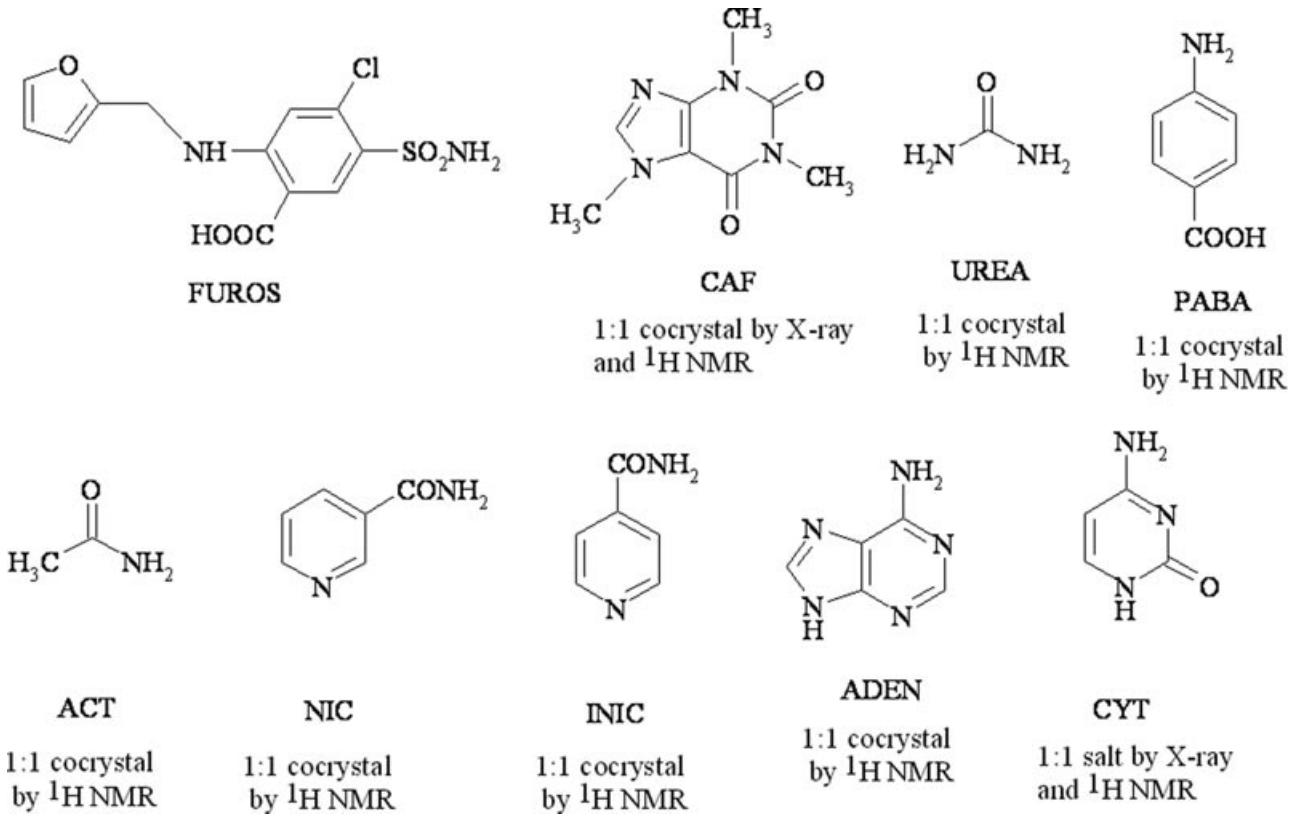

Scheme 1. Furosemide and coformers discussed in this study. The stoichiometry of furosemide–coformer cocrystal is indicated in each case along with the analytical method used. Compound abbreviations are used throughout the paper.

in all cases. Diffraction quality single crystals could be grown for FUROS–CAF and FUROS–CYT. The molecular composition and stoichiometry of these two cocrystals was unambiguously confirmed from their x-ray crystal structures. The nature of the cocrystal–salt continuum,[40] or the exact position of the H atom in an acid–base crystal structure, is sometimes difficult to ascertain except by accurate x-ray diffraction. Solid-state NMR[41] and XPS (x-ray photoelectron spectroscopy)[42] are complementary techniques to study the cocrystal/ salt state. FUROS–CAF was confirmed to be a cocrystal (neutral complex) and FUROS–CYT a salt (ionic structure) by x-ray crystallography. The exact location of the acidic hydrogen atom in other furosemide cocrystals could not be conclusively established due to nonavailability of single crystals for x-ray diffraction.

The structures of new multicomponent solid phases (i–viii) were confirmed by IR, NIR and Raman spectral analysis of the product cocrystals. This was followed by comparison of fingerprint lines in the PXRD patterns, which showed clear differences in 2θ values. A homogeneous cocrystal phase chemically different from the drug and the coformer was indicated by a sharp melting endotherm in DSC. The cocrystal composition was established, and stoichiometry was estimated by using ^{1}H NMR spectroscopy. Finally, solid-state ^{13}C NMR spectra were recorded to characterize all novel cocrystals. PXRD patterns, DSC thermograms, and ss-NMR spectra are presented in the paper, whereas IR, NIR, and Raman spectra are displayed in the Supporting Information. The structures of FUROS–CAF and FUROS–CYT determined to be cocrystal and salt, respectively, by x-ray crystallography are discussed first, followed by the remaining six cocrystals for which single crystal x-ray data are unavailable at the present time.

FUROS–CAF

Crystallization of a ground mixture of furosemide and caffeine from a MeOH–MeCN solvent mixture afforded diffraction quality single crystals, which solved and refined in the triclinic space group *P*-1 (Table 1). The crystal structure contains one molecule each of furosemide and caffeine in the asymmetric unit (Fig. S1), which confirms the cocrystal composition and stoichiometry. The most acidic COOH donor of furosemide is hydrogen bonded to the most basic N3 acceptor of caffeine via an O–H···N hydrogen bond (Fig. 1a). The primary sulfonamide NH donor hydrogen bonds to different caffeine C=O acceptor groups (Fig. 1b), and the secondary NH is bonded to one of the

Table 1. X-Ray Crystal Structure Data of Furosemide–Caffeine Cocrystal and Furosemide–Cytosine Salt

	FUROS–CAF	FUROS–CYT
Empirical formula	C_{20} H_{18} Cl N_6 O_7 S	C_{16} H_{16} Cl N_5 O_6 S
Formula weight	521.91	441.85
Crystal system	Triclinic	Triclinic
Space group	*P*-1	*P*-1
T (K)	100(2)	298(2)
a (Å)	7.512(2)	7.909(4)
b (Å)	9.462(3)	9.467(5)
c (Å)	17.198(5)	12.484(7)
α (°)	95.387(5)	100.151(8)
β (°)	102.271(5)	95.950(8)
γ (°)	110.101(5)	97.644(9)
Z	2	2
V (Å^3)	1103.0(6)	904.2(8)
Reflections collected	8290	9245
Unique reflections	4045	3489
Observed reflections	3388	3153
Parameters	363	290
R_1	0.0735	0.0390
wR_2	0.1874	0.1070
GOF	1.065	1.060
CCDC No.	833554	833555

sulfonyl O acceptors (Fig. 1c). Hydrogen bond metrics are listed in Table 2. The COOH group is in a neutral state (C=O 1.221(5) Å, C–O 1.315(5) Å), and the H atom is covalently bonded to the OH group and hydrogen bonded to the N acceptor (1.66 Å, 177°). The position of the acidic H atom was located in difference electron density maps. The purity of the bulk cocrystal phase was confirmed by an excellent overlay of the experimental PXRD pattern with the calculated lines from the x-ray crystal structure (Fig. 2). Thus a novel cocrystal of furosemide was obtained by liquid-assisted grinding,[43] and solution crystallization gave diffraction quality single crystals of the same compound. The furan moiety of furosemide was disordered in the crystal structure, determined at 100 K (Low Temperature (LT) structure). Since the pharmaceutical cocrystal composition is relevant at room temperature, we redetermined the structure at 298 K (Room Temperature (RT) structure). There was no change in the proton state (neutral O–H···N hydrogen bond) except that the disorder in the furan ring portion was too severe to assign partial occupancies in structure solution. The more accurate LT crystal structure is reported in this paper.

The carbonyl peak of furosemide occurs at 1673 ncm^{-1} in the IR spectrum and that of caffeine at 1658 and 1700 cm^{-1}; the peaks are shifted to 1699 and 1650 cm^{-1} in the cocrystal adduct. There are differences in the N–H stretching region between 3200 and 2500 cm^{-1}. The C=N stretch is shifted from 1658 cm^{-1} in caffeine to 1650 cm^{-1} in the cocrystal and the N–H bending vibration from 1592 cm^{-1} in furosemide to 1595 cm^{-1} in the product. IR, NIR, and Raman spectra details are presented in the Supporting Information (Tables S2, S3, and S4 and Figs. S2, S3, and S4).

Table 2. Hydrogen Bonds in Furosemide–Caffeine Cocrystal and Furosemide–Cytosine Salt Crystal Structures

Interaction	H···A (Å)	D···A (Å)	∠D–H···A (°)	Symmetry Code
FUROS–CAF				
O3–H3A···N3	1.66	2.642(3)	177	2–x, 1–y, 1–z
N1–H4A···O1	2.33	3.001(4)	139	x,–1+y, z
N1–H4A···O4	1.82	2.669(7)	123	Intramolecular
N2–H5A···O6	1.87	2.849(3)	164	1 + x, y, z
N2–H5B···O7	1.91	2.899(6)	166	1 + x, 1+ y, z
C1–H1B···N3	2.48	2.937(6)	104	Intramolecular
C1–H1B···O3	2.43	3.484(6)	165	2–x, 1–y, 1–z
C2–H2B···O6	2.31	2.726(5)	100	Intramolecular
C7–H7···O2	2.29	3.270(7)	149	2–x, 2–y, 1–z
C8–H8C···O1	2.30	3.190(7)	138	1+x, y, z
C11–H11···O5A	2.44	3.343(6)	140	Intramolecular
C14–H14···O2	2.32	2.790(7)	104	Intramolecular
FUROS–CYT				
N1–H1···O2	1.80	2.605(3)	134	Intramolecular
N2–H2A···Cl1	2.66	3.257(2)	118	Intramolecular
N2–H2A···O6	2.37	3.016(2)	121	1+x, y, z
N2–H2A···O5	2.44	3.349(9)	149	2–x,–y,–z
N5–H4···O3	1.83	2.828(8)	173	1–x,–y,–z
N5–H5···O3	1.89	2.849(2)	157	x, 1+y, z
N4–H6···O2	1.63	2.641(1)	178	1–x,–y,1–z
N3–H7···O6	1.85	2.857(8)	172	1–x,–y,–z
C2–H2···O4	2.38	2.842(7)	104	Intramolecular
C12–H12···O4	2.46	3.413(2)	146	x, 1+y, 1+z
C15–H15···O4	2.45	3.244(6)	129	x, 1+y, z

Neutron-normalized distances are used in the paper.

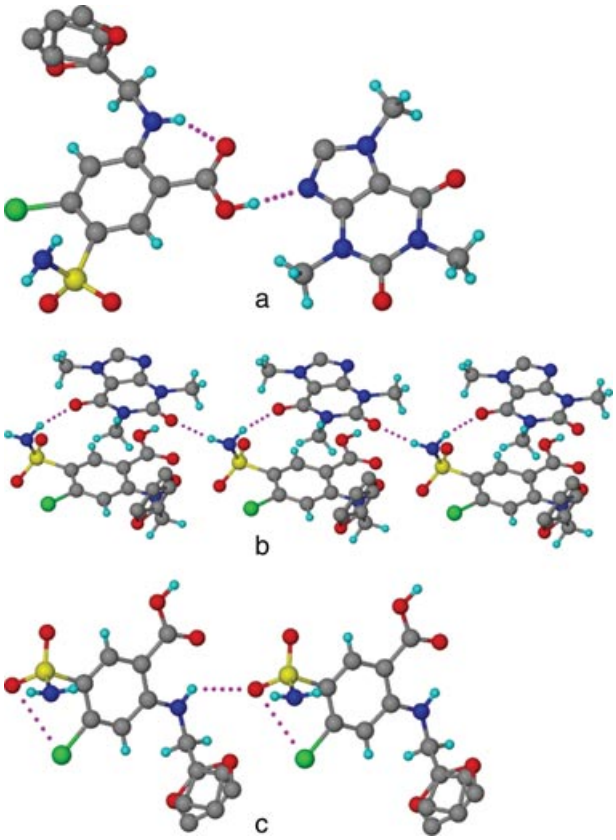

Figure 1. Hydrogen bonding in FUROS–CAF crystal structure. (a) COOH···N, (b) SO_2NH···O=C, and (c) NH···O_2S. The terminal furan ring is disordered over two sites with 0.65: 0.35 site occupancy factor of C18, C20, and O5 atoms in the low-temperature crystal structure data collected at 100 K.

The DSC thermogram (Fig. 3) of the cocrystal showed a single endotherm at a temperature different from that of the components (T_{peak} 225°C). The post-melting exotherm above 230°C is due to decomposition of furosemide to 4-chloro-5-sulfamoylanthranilic acid (saluamine) and other by-products upon heating (Scheme 2).[44] The single endotherm of the cocrystal is at a higher temperature than that of furosemide but lower than caffeine melting point. Furthermore, the DSC of the cocrystal did not exhibit small thermal events (e.g., polymorphic phase transitions), which were observed in DSC of commercial furosemide and caffeine. Melting data from DSC thermograms are summarized in Table 3.

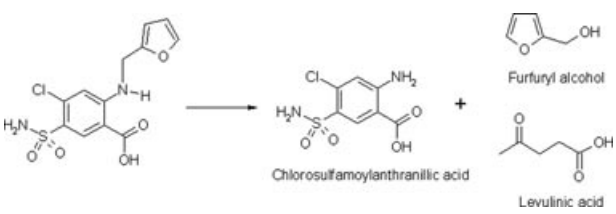

Scheme 2. Thermal degradation of furosemide to saluamine, furfuryl alcohol, and levulinic acid. This transformation occurs after melting of furosemide.

The solid-state ^{13}C NMR spectrum of the cocrystal showed peaks for furosemide plus caffeine, but the chemical shifts were moved upfield/downfield relative to the pure components. Since short-range aggregation and shielding/deshielding will be different in the starting components and product species, there are small but discernible chemical shift differences in the ss-NMR spectra (Fig. 4; see Table S5 for chemical shift values). The equimolar stoichiometry of FUROS—CAF cocrystal was confirmed by ^1H NMR integration (Fig. S5).

FUROS–CYT

Single crystals of furosemide–cytosine complex were obtained from MeOH solution. The x-ray crystal structure of FUROS–CYT was solved and refined in the triclinic space group *P*-1 (Table 1). The ORTEP diagram shows both the molecular components in the crystal lattice (Fig. S6). The main difference between this crystal structure and that of FUROS—CAF is that the proton is transferred from the COOH group of the drug to the basic N4 nitrogen of cytosine to make an ionic N—H^+···O^- hydrogen bond (1.63 Å, 178°). FUROS–CYT is a salt. The protonation state of the carboxylic acid and the basic nitrogen in acid–base structures can be difficult to predict a priori in cocrystal structures. There are several cases of borderline proton location and even a continuum of O···H···N hydrogen bond states was noted.[40,42,45] The electron density maps of x-ray diffraction showed that the acidic H atom is transferred and covalently bonded to the cytosine N and makes a hydrogen bond with the COO^- acceptor. The two C–O distances are nearly equal (1.247(2) Å, 1.262(2) Å) in the carboxylate group. Hydrogen bonding is mediated by the two-point carboxylate···aminopyridine synthon of $R^2_2(8)$ geometry.[46] Two furosemide molecules are hydrogen-bonded to two cytosine coformers via the carboxylate···amine $R^2_4(8)$ motif (Fig. 5). The cytosine molecules pair up via the carboxamide N—H···O dimer synthon. The bulk crystalline material prepared by liquid-assisted grinding matched with the single crystal phase purity (Fig. 6).

IR, Raman and NIR spectra (Figures S7, S8, and S9), DSC (Fig. 7), and NMR spectra (solid state in Fig. 8 and solution spectrum in Fig. S10) were satisfactory and consistent with the x-ray crystal structure analysis. DSC endotherms for the salt appeared at a different temperature from that for furosemide and the coformer (Table 3).

FUROS–UREA, FUROS–PABA, FUROS–ACT, FUROS–NIC, FUROS–INIC, and FUROS–ADEN

The next six cocrystal structures are described briefly because the same techniques were used

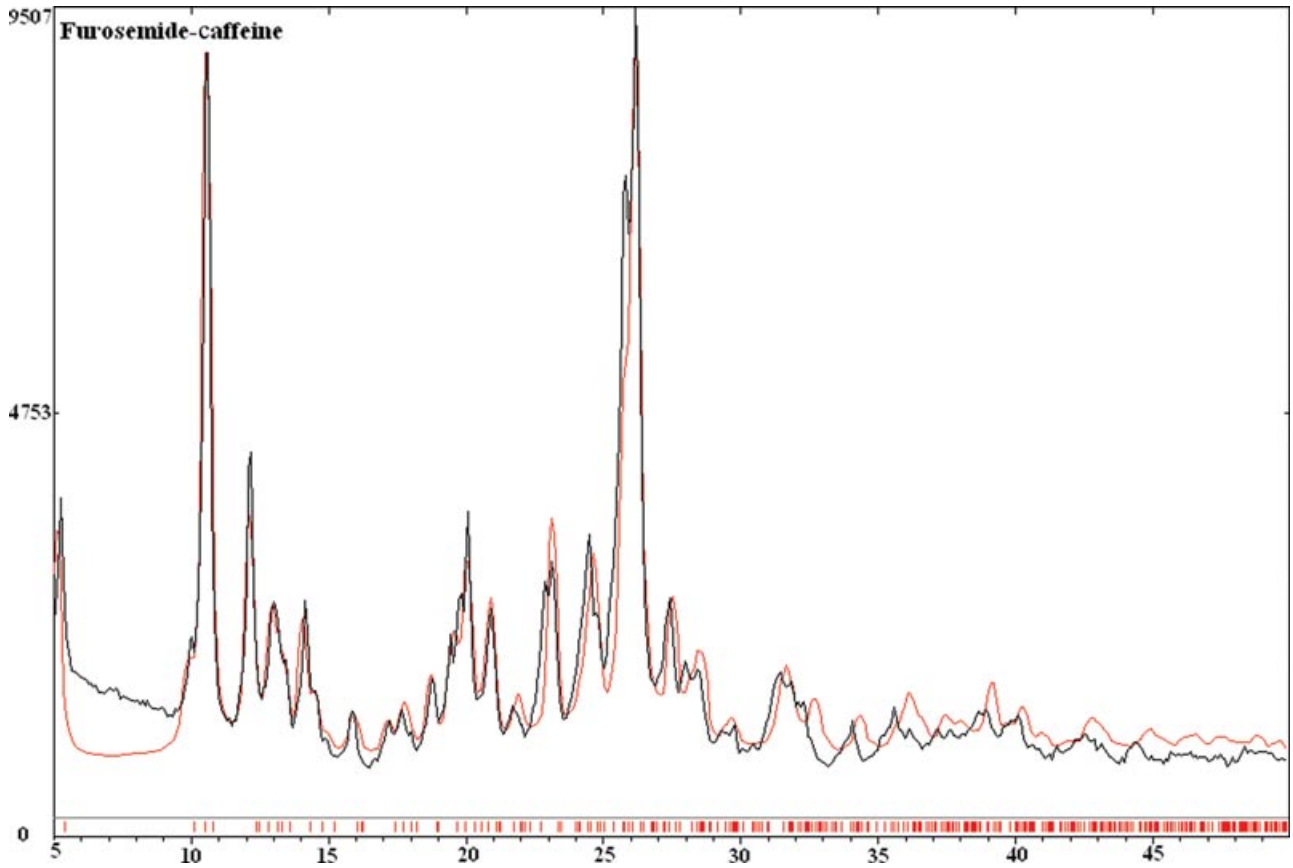

Figure 2. The experimental powder x-ray diffraction pattern of FUROS–CAF (black) and calculated lines from the crystal structure (red) show an excellent overlay in 2θ and reasonably good match of peak intensity. The small difference in peak position could be due to x-ray reflections being collected at 100 K and the PXRD was recorded at 300 K. Reitveld refinement gave $R_p = 0.1953$, $R_{wp} = 0.2500$, and $R_{exp} = 0.0257$.

as described above. That the structure and composition of furosemide–caffeine and furosemide–cytosine determined by several analytical methods[47] matched with the x-ray crystal structure in two cases gave us the confidence to characterize novel cocrystal phases, even in the absence of suitable single crystal data. Diffraction quality single crystals can be difficult to obtain for cocrystals, often due to mismatched solubility of the components, whereas microcrystalline powders are relatively easy to prepare by neat or liquid-assisted grinding.[48] The IR spectra of these six cocrystals (Fig. S11) showed significant differences compared to those of the drug and the coformer, providing evidence for new crystalline phases. Shifts in the CONH fragment of cocrystal spectra compared with components were observed in NH

Table 3. Melting Points of Furosemide Cocrystals Compared with Those of the Drug and Coformers Used

Drug/Coformer	Melting Point of Coformer[a] (°C)	Cocrystal/Salt	Melting Point of New Phase (°C)
FUROS	203	—	—
CAF[b]	227	FUROS–CAF	225
UREA	133	FUROS–UREA	156
PABA	187	FUROS–PABA	200
ACT (form 1, 2)	71, 81	FUROS–ACT	123
NIC[c] (form 1, 2)	106, 125	FUROS–NIC	150, 166
INIC (form 1, 2, 3)	161	FUROS–INIC	154, 196
ADEN	360	FUROS–ADEN	218
CYT	320	FUROS–CYT	232

[a] Multiple melting points are given for polymorphic compounds.
[b] Melting point of caffeine monohydrate is 234°C.
[c] At least six polymorphic forms of nicotinamide are reported by hot stage microscopy in Kofler L, Kolfer A. 1943., Chem Ber 76:246—248, having melting points (I) 129, (II) 110, (III) 113, (IV) 111, (V) 110, and (VI) 105°C. Melting points quoted in the table are taken from Li et al.[50]

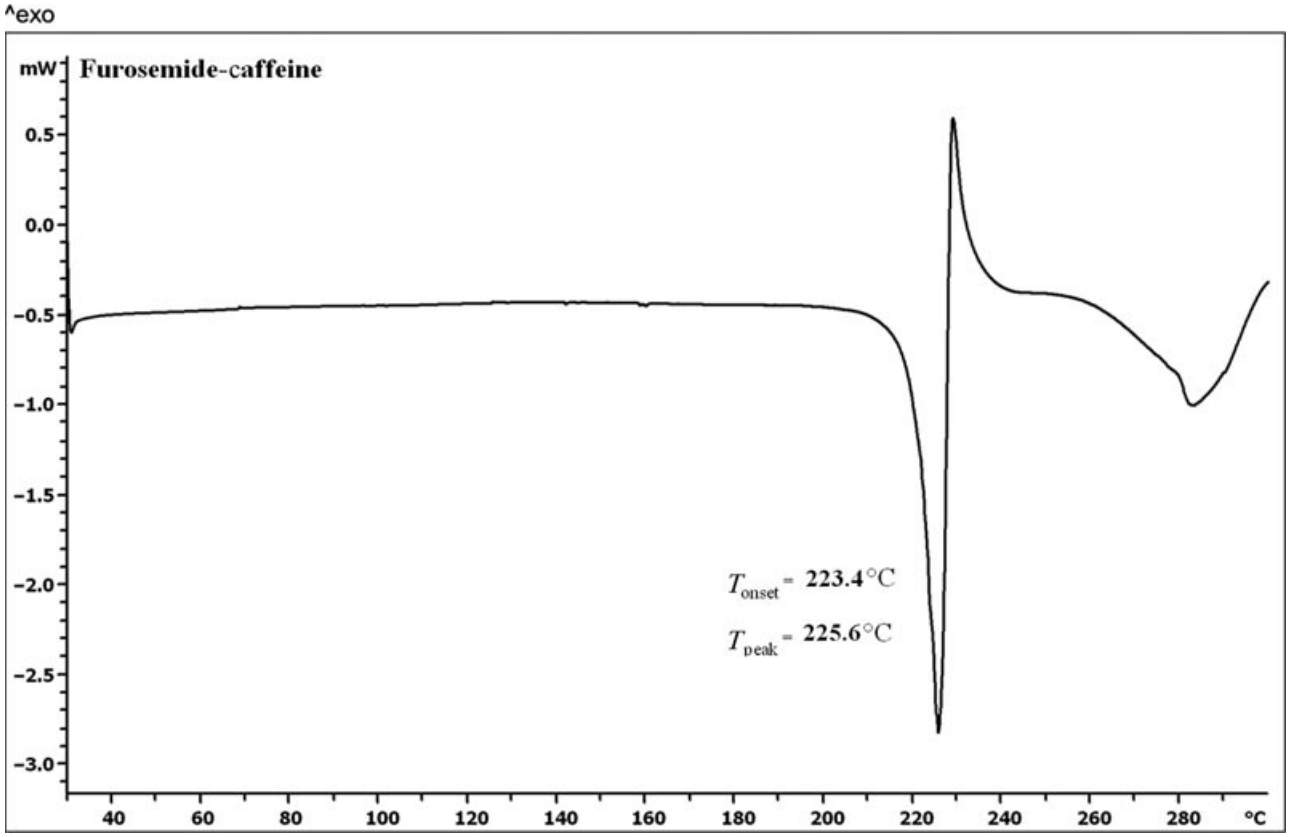

Figure 3. DSC thermogram of furosemide–caffeine cocrystal. The compound melts at 225°C (T_{peak}) followed by decomposition of furosemide between 227 and 240°C.Melting point of furosemide is 203–205°C and of caffeine is 227–228°C.

stretching and bending regions as well as for the carbonyl stretch peak, for example, in FUROS–UREA, FUROS–ACT, and FUROS–INIC. Their Raman and NIR spectra are compared in Figures S12 and S13 (in the Supporting Information). The melting point of the cocrystal was determined, and the phase purity was ascertained in DSC thermograms (Table 3; Fig. S14). All cocrystals exhibited sharp melting endotherms at temperatures significantly different from those for the drug and the coformer. The cocrystal melting point was lower than that of furosemide for urea, PABA (*p*-aminobenzoic acid), acetamide, nicotinamide, and isonicotinamide cocrystals but higher than the drug melting point for caffeine, adenine, and cytosine compounds. The intermediate melting point of furosemide cocrystals, that is in-between the drug and the coformer, is consistent with the general trend in cocrystals.[49] Multiple endotherms were observed for nicotinamide and isonicotinamide cocrystals, and a reason could be that polymorphs of the coformer are produced in the cocrystallization experiment by grinding. Polymorphs of nicotinamide and isonicotinamide[50] and multiple stoichiometries of their cocrystals were reported in recent studies.[51,52] The molecular composition of all the multicomponent phases and their stoichiometry were ascertained by ^{1}H NMR integration (Fig. S15). The analysis of nicotinamide and isonicotinamide cocrystals is complicated by the possibility of polymorphs and multiple stoichiometry. The 1:1 predominant cocrystal composition proposed is consistent with the available data.

Powder x-ray diffraction is a fingerprint technique to characterize the solid state. This is the most quantitative method for identifying novel crystalline phases when the x-ray crystal structure is not feasible due to microcrystalline nature of the sample. We observed new diffraction peaks in the powder XRD patterns of cocrystals compared with pure furosemide and the coformer (Fig. 9a). The calculated diffraction lines from x-ray crystal structures (Fig. 9b) are shown to detect the starting materials or polymorphic phases in the product cocrystal.

To confirm the cocrystal structure and composition, ^{13}C ss-NMR spectra[41] were recorded to discern short-range order differences and molecular mobility changes. The chemical shift values (δ scale) of ss-NMR spectra (Fig. 10) recorded at cross-polarization magic-angle spinning setting (CP-MAS) are convincing to confirm cocrystal formation. The δ values are presented in Table S5 for a detailed peak-by-peak comparison. The homogeneity of cocrystals and the absence of starting materials were established by ^{13}C

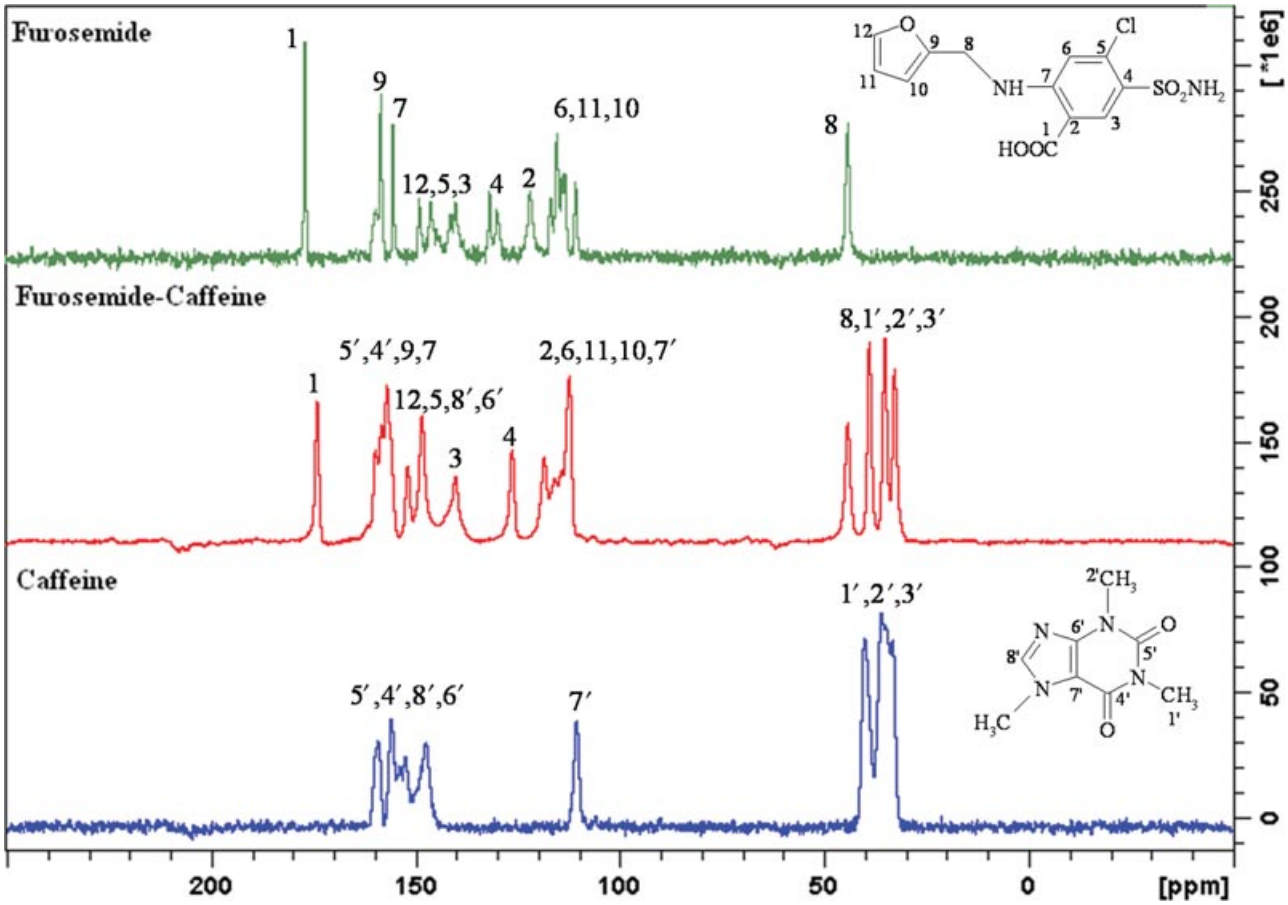

Figure 4. ^{13}C ss-NMR spectrum of FUROS–CAF cocrystal compared with the individual components.

ss-NMR spectra. A difference in the chemical shift peak positions of the cocrystal with respect to the individual components was considered as evidence for the formation of a new phase. For example, the carbonyl group of furosemide moved downfield in FUROS–UREA (δ 176.9–178.6) whereas the carbonyl group of urea moved upfield (δ 168.2–166.6), indicating a hydrogen-bonding interaction between the components. Similarly, carbonyl groups of furosemide and PABA were shifted in the cocrystal relative to the pure components. The carbonyl peaks in FUROS–ACT at (δ 174.7, 180.4) are shifted compared with individual resonances (δ 176.9, 181.5). Cocrystals of furosemide with nicotinamide, isonicotinamide, and adenine indicated new cocrystal phases by NMR.

Of eight molecular complexes prepared in this work, single crystals were obtained for two compounds. Furosemide–caffeine is a cocrystal and furosemide–cytosine is a salt. The structural details of the neutral or ionic state were known after single crystal x-ray diffraction. Surprisingly, the IR spectrum of furosemide–cytosine did not exhibit a broad carboxylate band at 1600–1650 cm^{-1} and a sharper peak for the carboxylic acid group at 1700 cm^{-1} for furosemide–caffeine. The fact that the multicomponent systems are also multifunctional (COOH/COO^-, CONH) makes it difficult to assign the carbonyl peaks individually. Whereas normally it is relatively easy to differentiate between COOH and COO^- by IR spectroscopy, it would have been difficult to make the same assignment for the above-discussed cocrystal/salt without knowledge of the x-ray crystal structures. The carbonyl resonance occurred between δ 160 and 170 ppm in the NMR spectra for furosemide whether the molecule is in the neutral (COOH) or ionized (COO^-) state. ^{15}N ss-NMR[41] and XPS[42] should unequivocally clarify the cocrystal/salt nature of all the furosemide adducts, and these measurements will be carried out to clarify the ionization state. The main objective of this preliminary study was to search for novel solid-state forms of furosemide with GRAS coformers to discover crystalline materials of improved solubility and stability.

The melting endotherms in DSC for cocrystals are sharp and occur in-between the furosemide and the coformer (Table 3). This indicated cocrystal formation.[49] We believe that the examples discussed in this paper are cocrystals, not eutectic compositions. Generally, the melting point of eutectic is lower than either of the components and, moreover,

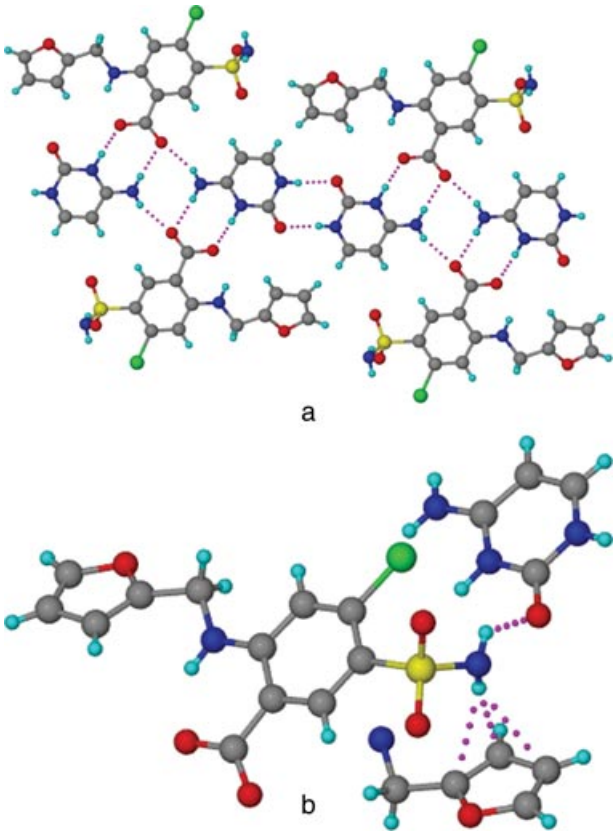

Figure 5. X-ray crystal structure of FUROS–CYT salt. (a) $R^2_2(8)$ and $R^2_4(8)$ N—H···O hydrogen bond ring motifs. (b) The SO_2NH_2 group donors engage in N—H···O and N—H···π(furan) hydrogen bonds.

it does not depend on the stoichiometry in which the components were mixed or reacted. This was not the case for furosemide cocrystals. Another indication for cocrystal instead of the eutectic phase is the stability experiments (discussed next). The PXRD of the stable cocrystals in this study, that is furosemide–caffeine, furosemide–adenine, and furosemide–cytosine, matched with those of the product solid forms, but not with the individual components. This implies that a novel crystalline adduct is present, not a eutectic phase. A physical mixture would have shown PXRD lines matching with those of the starting materials after the slurry experiment.

Solubility and Dissolution

Solubility and intrinsic dissolution rate (IDR) were determined on a *U.S. Pharmacopeia* (USP) approved dissolution tester.[53,54] A typical measurement is described in the Experimental section. Solubility is the concentration of a substance in the solvent when the dissolved and undissolved particles are in a state of dynamic equilibrium. Solubility is a thermodynamic quantity and usually taken as the concentration of the solute at 24 or 48 h after mixing in a solvent. The solubility measurement is unsuited for those drug forms that are metastable and undergo phase transformation during the slurry conditions of dissolution. The rate at which the equilibrium solubility is reached is the dissolution rate, which is a kinetic parameter. The IDR method overcomes the problems of drug particle size and morphology effects. Dissolution rate studies rely on the supersaturation phenomenon, that is the peak concentration of the drug delivered through a suitable carrier (e.g., amorphous, salt, cocrystal, nanoparticle)[55] in a short period of time (say 2–4–6 h) depending on the stability of the drug form being tested. The survival of the starting drug form during the course of the test conditions and until the end of the experiment must be verified independently, usually by PXRD or video microscopy. IDR measures the rate of drug dissolution from a constant surface area of the disk in a unit time. Because of the very low solubility of furosemide in aqueous medium, all dissolution and solubility experiments were carried out in 10% ethanol–water (Fig. 11).

The drug concentration was determined by UV–vis spectroscopy from a calibrated concentration–intensity curve. Furosemide shows maxima of decreasing intensities at 230 nm, 275 nm, and a third shallow, broad maximum at 335 nm. Among the coformers in this study, caffeine, cytosine, and *p*-aminobenzoic acid absorb between 240 and 300 nm but they exhibit no maxima beyond this region even at the highest concentration considered. There is a slight up-curve above the base line at 230–240 nm due to the coformer peaks, but this small contribution is no more than 10% (Fig. S16). This artifact can be corrected using the drug:coformer concentration calibration curves. To minimize possible errors due to overlapping peaks, the maximum in furosemide UV–vis spectrum at 335 nm was used to calculate drug concentrations without any interference from coformer peaks.

The solubility of the drug and cocrystal powders was determined at 24 h. Apart from furosemide, which was stable to the slurry conditions, furosemide–caffeine, furosemide–adenine, and furosemide–cytosine were stable for the same period (Fig. S17); there was no perceptible change in the PXRD pattern even up to 48 h. The solubility of all cocrystals is superior to that of the pure drug. The other five cocrystals with urea, PABA, acetamide, nicotinamide, and isonicotinamide converted to furosemide within 24 h. The solubility order for the stable cocrystals (no phase transformation observed) is furosemide–cytosine > furosemide–adenine > furosemide–caffeine > furosemide, which have 11, 7, and 6 times higher solubility than furosemide. The dissolution rate advantage is modest (about twofold faster). Since there is no evidence of the solid-form conversion for extended periods of time, the solubility numbers may be used as a safe guide to estimate the higher aqueous exposure and bioavailability of

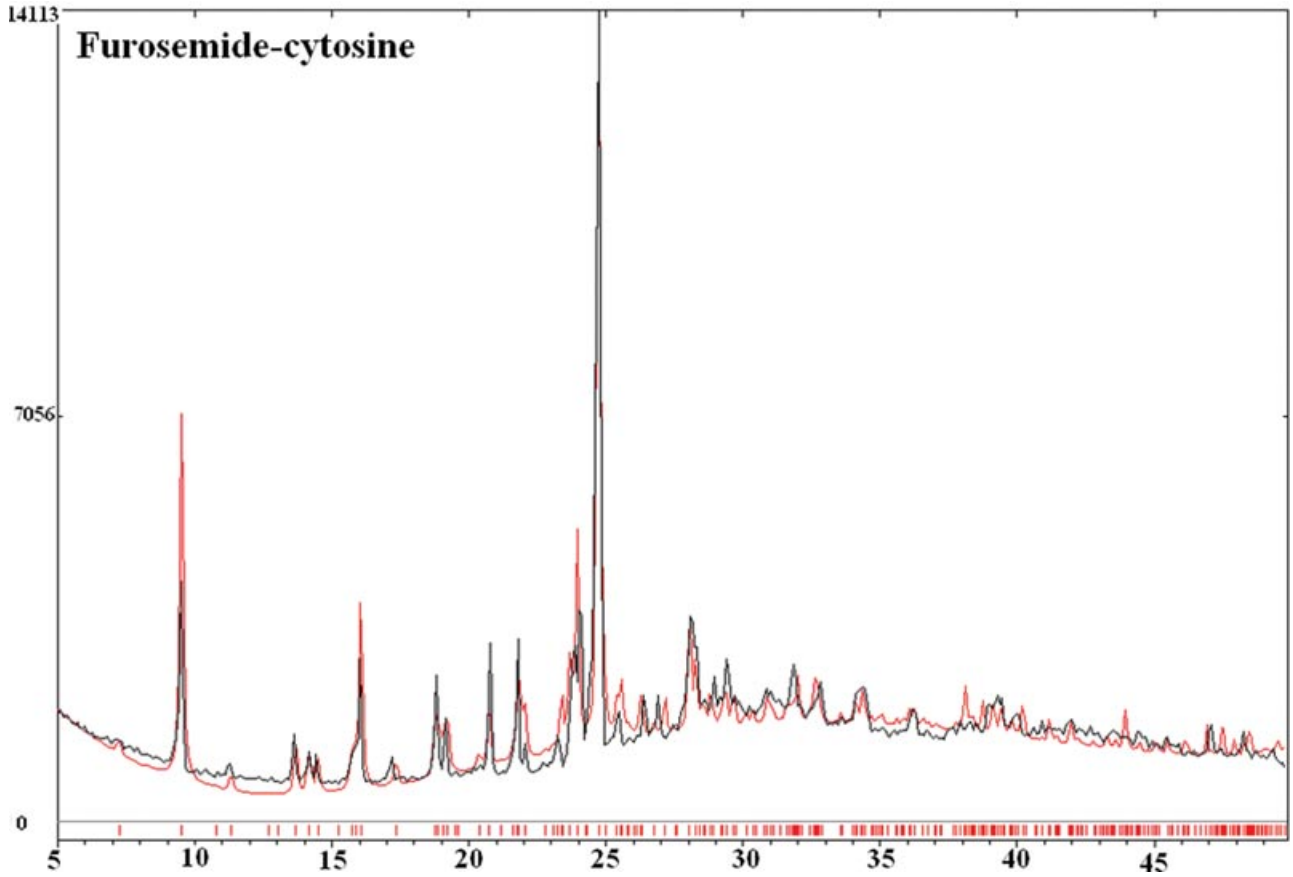

Figure 6. Experimental PXRD of FUROS–CYT (black trace) overlaid on the calculated diffraction lines from the x-ray crystal structure (red). The matching of the bulk material with the single crystal phase is excellent. Reitveld refinement gave $R_p = 0.1833$, $R_{wp} = 0.2514$, and $R_{exp} = 0.0270$.

cocrystals compared with the pure drug. The equilibrium solubility at 24 h and the dissolution rate from the linear region of the IDR curve are presented in Table 4.

The reasons for solubility enhancement may be described on the basis of the solubility of the coformer in water (Table 4) and from crystal structure analysis (Figs. 1 and 5). The high solubility of FUROS–NIC cocrystal is not surprising[56] because nicotinamide is one of the highest soluble coformers that is used in pharmaceutical cocrystallization. Hence the highly soluble coformer guides the high concentration of the drug cocrystal.[57,58] However, this explanation, which is based on the linear relationship between the solubility ratio of the components plotted against the solubility of the former cocrystal divided by the solubility of the API (Active Pharmaceutical Ingredient),[57] has its limitations. The above model is faithfully realized only when the cocrystals whose solubility is being compared have similar hydrogen bonding and molecular packing. For example, the highest solubility of FUROS–CYT does not correlate with the low solubility of cytosine. On the other hand, FUROS–CAF has lower solubility even though caffeine is more soluble. A reason for these observations is that there are drastic changes in the crystal structure and hydrogen bonding from neutral to ionic in FUROS–CAF and FUROS–CYT. We believe that the salt nature of the latter compound guides its highest aqueous solubility. The solubility data of Table 4 indicate that FUROS–CAF, FUROS–ADEN, and FUROS–CYT are congruently dissolving systems because they are pairs of similar solubility. The other systems are incongruently dissolving due to the huge difference in their components solubilities.[59,60] Their stabilities are consequently related. Congruent systems tend to be more stable in the slurry medium. In incongruent systems, however, the highly soluble coformer causes rapid dissolution and dissociation of the cocrystal to its components. FUROS–PABA is an exception to the above-mentioned analysis.

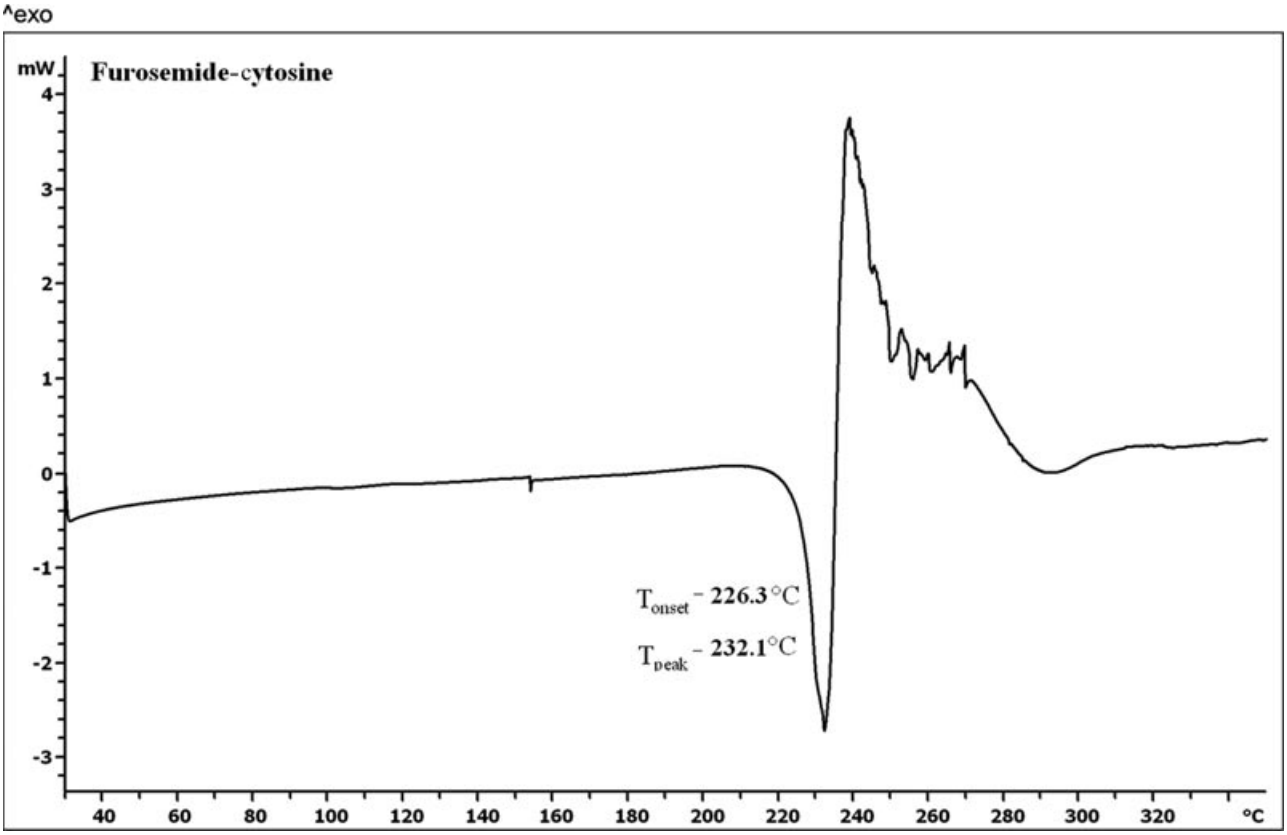

Figure 7. DSC of FUROS–CYT. The salt exhibits a melting endotherm at 232°C (T_{peak}) followed by decomposition of furosemide between 240 and 260°C. Melting point of furosemide is203–205°C and of cytosine is 320–322°C.

CONCLUSIONS

Solid-state crystalline forms of an insoluble antihypertensive drug furosemide were prepared using liquid-assisted grinding and slurry methods. Single crystal x-ray structure validation was performed on two of eight materials. All the products were characterized by DSC, ss-NMR, PXRD, IR, NIR, and Raman measurements. Even as crystal engineering principles offer guidelines for the rational selection of coformers for a particular API, the exact cocrystal structure and the neutral/ionic state of the product are difficult to know without a crystal structure. Structure solution from powder diffraction data is still not a routine method for large and flexible molecules. Furosemide–caffeine is a cocrystal, and furosemide–cytosine is a salt as revealed by x-ray crystal structure analysis. A definitive answer about the neutral/ionic state of other six furosemide compounds is pending upto the availability of XPS/NMR measurements or good quality single crystals. A practical advantage that cocrystals offer over metastable

Table 4. Solubility and IDR in 10% Ethanol–Water

Compound	Solubility at 24 h in 10% EtOH–Water (mg/L)	Solubility in Water (mg/mL)	Intrinsic Dissolution Rate in 10% EtOH–Water (mg/cm^2)/min	Stability in 10% EtOH–Water Slurry Medium
FUROS	118	0.006	44×10^{-3}	Stable after 24, 48 h
FUROS–CAF	720 (×6.1)	22	87×10^{-3} (×1.9)	Stable after 24, 48 h
FUROS–UREA	632 (×5.3)	1000	83×10^{-3} (×1.9)	Converted to furosemide within 24 h
FUROS–PABA	370 (×3.1)	5	53×10^{-3} (×1.2)	Converted to furosemide within 24 h
FUROS–ACT	812 (×6.9)	2000	94×10^{-3} (×2.1)	Converted to furosemide within 24 h
FUROS–NIC	1040 (×8.8)	1000	111×10^{-3} (×2.5)	Converted to furosemide within 24 h
FUROS–INIC	856 (×7.2)	192	102×10^{-3} (×2.3)	Converted to furosemide within 24 h
FUROS–ADEN	787 (×6.7)	9	91×10^{-3} (×2.1)	Stable after 24, 48 h
FUROS–CYT	1260 (×10.7)	8	116×10^{-3} (×2.6)	Stable after 24, 48 h

Numbers in parentheses give the number of times solubility is higher compared to the pure drug.
Solubility of the coformer is given in water.
The stable cocrystal entries are highlighted in bold.

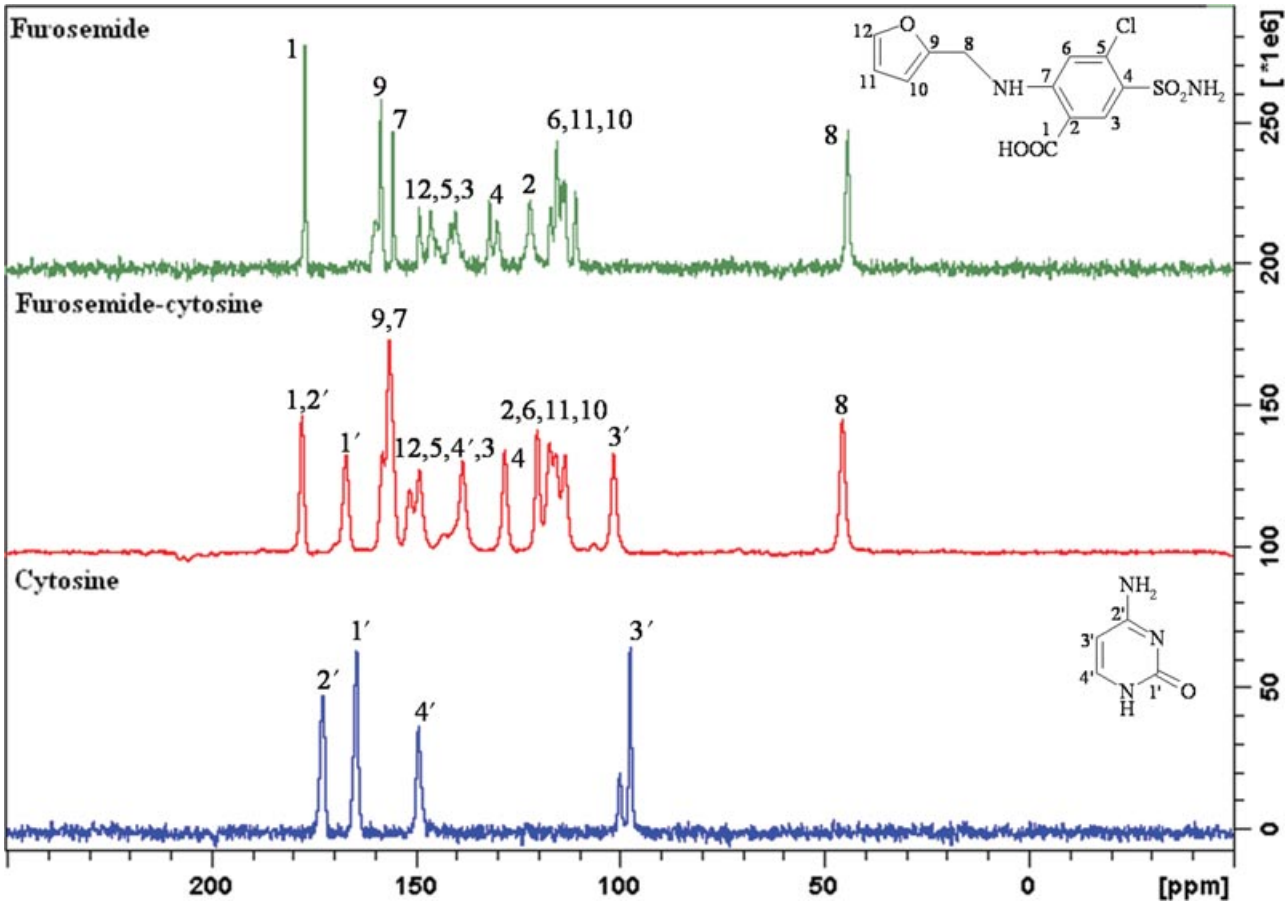

Figure 8. ^{13}C ss-NMR of FUROS–CYT and the individual components show that a novel solid-state complex was formed upon grinding.

polymorphs or amorphous drug forms is that they are relatively more stable owing to their crystalline nature. Thus cocrystals can combine the twin aspects of improved solubility and good stability for optimal drug delivery. Furosemide–caffeine, furosemide–adenine, and furosemide–cytosine exhibited comparable stability to the commercial drug in 10% ethanol–water slurry medium up to 48 h. Moreover, their solubility is 6–11-fold higher relative to furosemide. Thus cocrystals could offer a superior strategy to improve the solubility of BCS class II/IV drugs compared to metastable polymorphs and amorphous dispersions.

EXPERIMENTAL

Furosemide (purity >99.8%) was supplied by AstraZeneca India Pvt. Ltd (Bangalore, India). Coformers (purity >99.8%) were purchased from Sigma-Aldrich (Hyderabad, India). Solvents (purity >99%) were purchased from Hychem Laboratories (Hyderabad, India). Water filtered through a double deionized purification system (AquaDM, Bhanu, Hyderabad, India) was used in all experiments.

Preparation of Furosemide Cocrystals

Furosemide (34 mg) and caffeine (20 mg) (1:1 molar ratio) were ground and mixed in a mortar–pestle for 20 min after adding 5–6 drops of acetonitrile, a liquid-assisted grinding procedure. Cocrystal formation was confirmed by changes in the signature peaks of FT-IR and PXRD. Forty milligram of the ground material was dissolved in 5 mL of MeOH–CH_3CN solvent mixture and left aside for evaporation at ambient conditions. Single crystals suitable for x-ray diffraction appeared after 4–5 days.

Furosemide (68 mg) and urea (12 mg) (1:1 molar ratio) were ground and mixed together in a mortar–pestle for 20 min after adding 5–6 drops of acetone, a liquid-assisted grinding procedure. Cocrystal formation was confirmed by changes in the signature peaks of FT-IR and PXRD.

Furosemide (34 mg) and *p*-aminobenzoic acid (14 mg) (1:1 molar ratio) were ground and mixed in a mortar–pestle for 20 min after adding 5–6 drops of acetone, a liquid-assisted grinding procedure. Cocrystal formation was confirmed by changes in the signature peaks of FT-IR and PXRD. The same cocrystal was also obtained by using the slurry

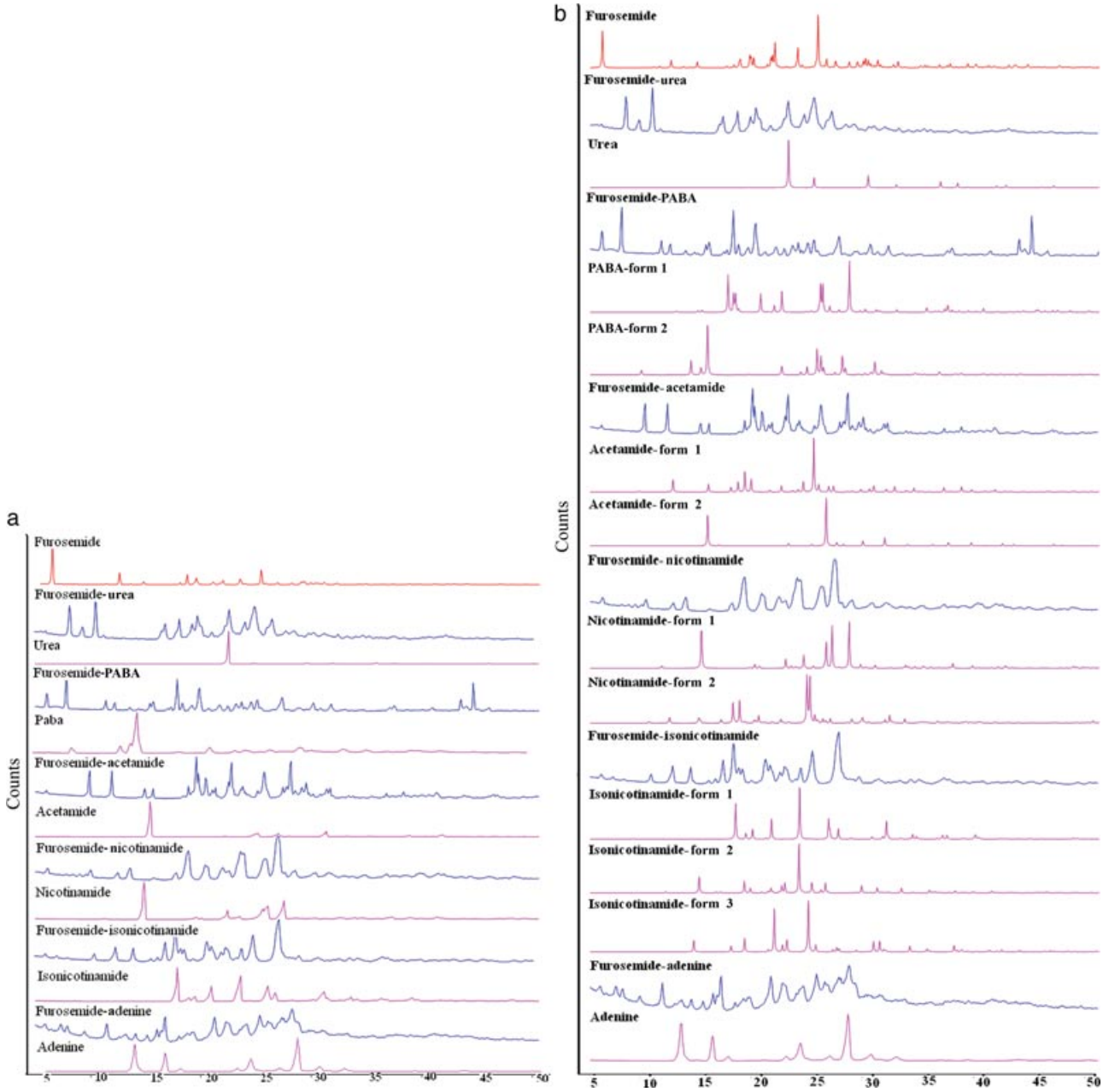

Figure 9. (a) Experimental PXRD plots of furosemide, cocrystal, and coformer to compare 2θ values in the new crystalline phases. (b) Calculated PXRD lines form the x-ray crystal structure for furosemide, coformer polymorphs, and cocrystals for fingerprint matching of starting materials in the product phases of (a).

crystallization method. PABA (14 mg) was dissolved in 1.5-mL MeOH and 3.5 mL of H_2O, and furosemide (34 mg) was added with stirring. The formation of cocrystal was completed after 30 min.

Furosemide (68 mg) and acetamide (12 mg) (1:1 molar ratio) were ground and mixed in a mortar–pestle for 20 min after adding 5–6 drops of acetonitrile, a liquid-assisted grinding procedure. Cocrystal formation was confirmed by changes in the signature peaks of FT-IR and PXRD.

Furosemide (34 mg) and nicotinamide (13 mg) (1:1 molar ratio) were ground and mixed in a mortar–pestle for 20 min after adding 5–6 drops of acetone, a liquid-assisted grinding procedure. Cocrystal formation was confirmed by changes in the signature peaks of FT-IR and PXRD.

Furosemide (34 mg) and isonicotinamide (13 mg) (1:1 molar ratio) were ground and mixed in a mortar–pestle for 20 min after adding 5–6 drops of acetone, a liquid-assisted grinding procedure. Cocrystal

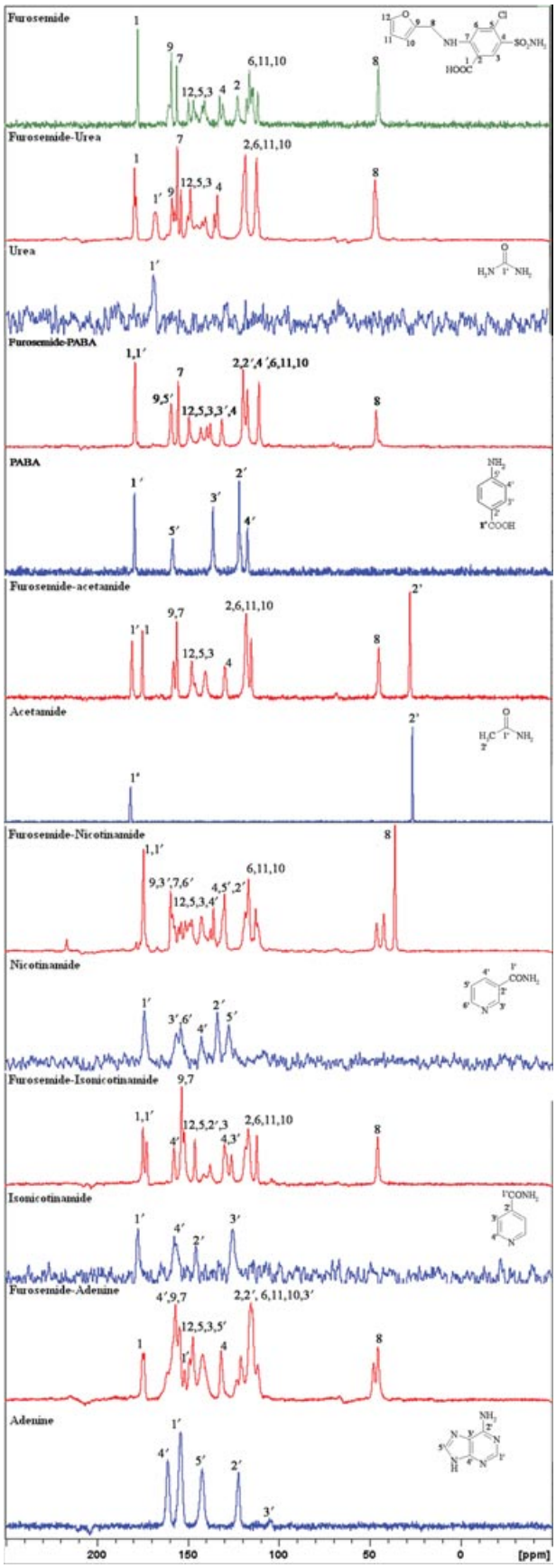

Figure 10. ^{13}C ss-NMR spectra of cocrystals, drug, and coformers.

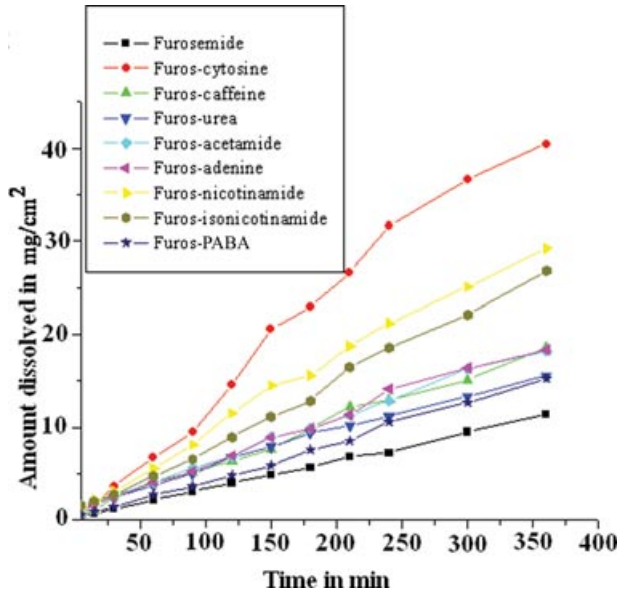

Figure 11. Dissolution curve of furosemide and its cocrystals for up to 6 h.

formation was confirmed by changes in the signature peaks of FT-IR and PXRD.

Furosemide (34 mg) and adenine (14 mg) (1:1 molar ratio) were ground and mixed in a mortar–pestle for 20 min after adding 5–6 drops of acetone, a liquid-assisted grinding procedure. Cocrystal formation was confirmed by changes in the signature peaks of FT-IR and PXRD. The same cocrystal was also obtained by the slurry crystallization method. Furosemide (110 mg) and adenine (40 mg) was added to 8-mL MeOH with stirring. The formation of cocrystal was complete after 7–8 h.

Furosemide (34 mg) and cytosine (12 mg) (1:1 molar ratio) were ground and mixed in a mortar–pestle for 20 min after adding 5–6 drops of acetonitrile, a liquid-assisted grinding procedure. Cocrystal formation was confirmed by changes in the signature peaks of FT-IR and PXRD. Fifty milligram of the ground material was dissolved in 6 mL of MeOH and left aside for evaporation at ambient conditions. Single crystals suitable for x-ray diffraction appeared after 5–6 days.

Vibrational Spectroscopy

A Thermo-Nicolet 6700 Fourier transform infrared spectrophotometer with an NXR-Fourier transform Raman module (Thermo Scientific, Waltham, MA) was used to record IR, Raman, and NIR spectra. IR and NIR spectra were recorded on samples dispersed in KBr pellets. Raman spectra were recorded on samples contained in standard NMR diameter tubes or on compressed samples contained in a gold-coated sample holder. Data were analyzed using the Omnic software (Thermo Scientific, Waltham, MA).

Solid-State NMR Spectroscopy

Solid-state ^{13}C NMR spectra were obtained on a Bruker Avance 400 MHz spectrometer (Bruker-Biospin, Karlsruhe, Germany). Ss-NMR measurements were carried out on Bruker 4-mm double resonance CP-MAS probe in zirconia rotors with a Kel-F cap at 5.0-kHz spinning rate with a cross-polarization contact time of 2.5 ms and a delay of 8 s. ^{13}C NMR spectra were recorded at 100 MHz and referenced to the methylene carbon of glycine ($\delta_{glycine} = 43.3$ ppm).

Thermal Analysis

Differential scanning calorimetry was performed on a Mettler-Toledo DSC 822e module, and TGA was performed on a Mettler Toledo TGA/SDTA 851e module (Mettler-Toledo, Columbus, OH). Samples were placed in sealed pin-pricked alumina pans for TG experiments and in crimped but vented aluminum pans for DSC experiments. The typical sample size is 3–5 mg for DSC and 8–12 mg for TGA. The temperature range for the thermogram was 30–300°C, and the sample was heated at a rate of 5°C/ min. Samples were purged in a stream of dry nitrogen flowing at 80 mL/min for DSC and 50 mL/min for TGA. The TGA of FUROS–UREA and FUROS–ACT is shown as representative cases of cocrystals (Fig. S18) to monitor the decomposition of furosemide in the postmelting stage.

Powder X-Ray Diffraction

Powder x-ray diffraction of all the samples was recorded on a Bruker D8 advance diffractometer (Bruker-AXS, Karlsruhe, Germany) using Cu Kα x-radiation ($\lambda = 1.5406$ Å) at 40 kV and 30 mA power. X-ray diffraction patterns were collected over the 2θ range 5–50° at a scan rate of 1°/min. Powder Cell 2.4[61] (Federal Institute of Materials Research and Testing, Berlin, Germany) was used for Rietveld refinement of experimental PXRD and calculated lines from the x-ray crystal structure. The calculated crystal structures of coformer polymorphs not determined in this study were taken from the literature[50] or extracted from the CCDC (Cambridge Crystallographic Data Centre).[62]

X-Ray Crystallography

X-ray reflections were collected on a Bruker Smart-Apex CCD diffractometer (Bruker-AXS, Karlsruhe, Germany). Mo Kα x-radiation ($\lambda = 0.71073$ Å) was used to collect x-ray reflections on the single crystal. Data reduction was performed using the Bruker SAINT software.[63] Intensities for absorption were corrected using SADABS,[64] the Siemens area detector absorption correction program (Bruker-AXS). Crystal structures were solved and refined using SHELX-97[65] with anisotropic displacement parameters for non-H atoms. Hydrogen atoms on O and N were experimentally located in difference electron density maps. All C—H atoms were fixed geometrically using HFIX command in SHELX-TL (Bruker-AXS). A check of the final CIF file using PLATON[66] did not show any missed symmetry. Hydrogen bond distances shown in Table 2 are neutron normalized to fix the D–H distance to its accurate neutron value in the x-ray crystal structures (O–H 0.983 Å, N–H 1.009 Å, and C–H 1.083 Å). X-Seed[67] was used to prepare packing diagrams. Crystallographic.cif files (CCDC Nos. 833554–833555) are available at www.ccdc.cam.ac.uk/data or as part of Supporting Information.

Dissolution and Solubility Measurements

The solubility of furosemide and its cocrystals were determined according to the Higuchi and Connor method[68] in 10% ethanol–water medium at 30°C. First, the absorbance of a known concentration of the cocrystal/drug was measured at the respective λ_{max} (furosemide 334 nm, furosemide–caffeine 330 nm, furosemide–urea 331 nm, furosemide–PABA 331 nm, furosemide–acetamide 330 nm, furosemide–nicotinamide 330 nm, furosemide–isonicotinamide 329 nm, furosemide–adenine 330 nm) in 10% ethanol–water medium on a Thermo Scientific Evolution 300 UV–vis spectrometer (Thermo Scientific, Waltham, MA). These absorbance values were plotted against several known concentrations to prepare the concentration versus intensity calibration curve. From the slope of the calibration curves, molar extinction coefficients (Table S6) for the cocrystal/drug were calculated. An excess amount of the sample was added to 6 mL of 10% ethanol–water medium. The supersaturated solutions were stirred at 300 rpm using a magnetic stirrer at 30°C. After 24 h, the suspension was filtered through Whatman's filter paper No. 1. The filtered aliquots were diluted sufficiently, and the absorbance was measured at the respective λ_{max}. Finally, the concentrations of furosemide and its cocrystals were calculated at regular time intervals of 24 and 48 h using the relevant calibration curve. IDR experiments were carried out on a USP-certified Electrolab TDT-08L dissolution tester (Mumbai, India). Dissolution experiments were performed for 6 h in 10% ethanol–water medium at 37°C. Prior to IDR estimation, standard curves for all the compounds were obtained spectrophotometrically at their respective λ_{max}. The respective molar extinction coefficients were used to determine the IDR values. For IDR measurements, 100 mg of the compound was taken in the intrinsic attachment and compressed to a 0.5-cm^2 disk using a hydraulic press at pressure of 4.0 ton/ $in.^2$ for 5 min. The intrinsic attachment was placed in a jar of 500-mL medium preheated to 37°C and rotated at 150 rpm. Five milliliter of aliquot was collected at specific time intervals, and the concentration of the aliquots was determined with appropriate

dilutions from the predetermined standard curves of the respective compounds. The IDR of the compound was calculated in the linear region of the dissolution curve (which is the slope of the curve or amount of drug dissolved/surface area of the disk) per unit time. The identity of the undissolved material after the dissolution experiment was ascertained by PXRD. The stability of the solid samples after disk compression and solubility measurements was confirmed by PXRD.

ACKNOWLEDGMENTS

AN thanks the Department of Science and Technology, Government of India (DST) for research funding (SR/S1/OC-67/2006) and J.C. Bose fellowship (SR/S2/JCB-06/2009) and Council of Scientific and Industrial Research (CSIR) project (01/2410)/10/EMR-II). DST (IRPHA) and University Grants Commission (UGC) (PURSE grant) are thanked for providing instrumentation and infrastructure facilities at University of Hyderabad (UOH). NRG thanks CSIR, and KS thanks UGC for a fellowship. Crystalin Research Pvt. Ltd. (Hyderabad, India) thanks AstraZeneca Pvt. Ltd. (Bangalore, India) for funding a research project. We thank Dr. Mike Quayle and Dr. David Berry (AstraZeneca PLC) for their critical comments and helpful suggestions. This publication is assigned AstraZeneca ATP No. 11/1199.

REFERENCES

1. Qiu Y, Chen Y, Zhang GGZ., Eds. 2009. Developing solid oral dosage forms: Pharmaceutical theory and practice, 1st ed. New York: Academic Press.
2. Thayer AM. 2010. Finding solutions. Chem Eng News 88:13–18.
3. Amidon GL, Lennernas H, Shah VP, Crison JR. 1995. Theoretical basis for a biopharmaceutical drug classification: correlation of in vitro drug product dissolution and in vivo bioavailability. Pharm Res 12:413–420.
4. Dahan A, Miller JM, Amidon GL. 2009. Prediction of solubility and permeability class membership: Provisional BCS classification of world's top oral drugs. AAPS J 11:740–746.
5. Friedman PA, Berndt WO. 1997. In Modern pharmacology with clinical applications; Craig CR, Stitzel RE, Eds. 5th ed. Boston, MA: Little Brown and Company, pp 239–255.
6. Khan MG. 2006. Encyclopedia of heart diseases. 15th ed.New York: Elsevier, pp 486.
7. Blagden N, de Matas M, Gavan PT, York P. 2007. Crystal engineering of active pharmaceutical ingredients to improve solubility and dissolution rates. Adv Drug Del Rev 59:617–630.
8. Shan N, Zaworotko MJ. 2008. The role of cocrystals in pharmaceutical science. Drug Discov Today 13:440–446.
9. Doherty C, York P. 1988. Furosemide crystal forms: Solid state and physicochemical analyses. Int J Pharm 47:141–155.
10. Matsuda Y, Tatsumi E. 1990. Physicochemical characterization of furosemide modifications. Int J Pharm 60:11–26.
11. Ge M, Liu G, Ma S, Wang W. 2009. Polymorphic forms of furosemide characterized by THz time domain spectroscopy. Bull Korean Chem Soc 30:2265–2268.
12. Karami S, Li Y, Hughes DS, Hursthouse MB, Russell AE, Threlfall TL, Claybourn M, Roberts R. 2006. Further errors in polymorph identification: Furosemide and finasteride. Acta Crystallogr B 62:689–691.
13. Babu NJ, Cherukuvada S, Thakuria R, Nangia A. 2010. Conformational and synthon polymorphism in furosemide (Lasix). Cryst Growth Des 10:1979–1989.
14. Ai H, Jones SA, deVilliers MM, Lvov YM. 2003. Nano encapsulation of furosemide microcrystals for controlled drug release. J Control Release 86:59–68.
15. Matsuda Y, Otsuka M, Onoe M, Tatsumi E. 1992. Amorphism and Physicochemical stability of spray-dried frusemide. J Pharm Pharmacol 44:627–633.
16. Shin SC, Oh IJ, Lee YB, Choi HK, Choi JS. 1998. Enhanced dissolution of furosemide by coprecipitating or cogrinding with crospovidone. Int J Pharm 175:17–24.
17. Shin SC, Kim J. 2003. Physicochemical characterization of solid dispersion of furosemide with TPGS. Int J Pharm 251:79–84.
18. Özdemir N, Ordu S. 1998. Improvement of dissolution properties of furosemide by complexation with β-cyclodextrin. Drug Dev Ind Pharm 24:19–25.
19. Kreaz RMA, Abu-Eida EY, Erős I, Kata M. 1999. Freeze dried complexes of furosemide with β-cyclodextrin derivatives. J Incl Phenom Macrocycl Chem 34:39–48.
20. Wongmekiat A, Yoshimatsu S, Tozuka Y, Moribe K, Yamamoto K. 2006. Investigation of drug nanoparticle formation by cogrinding with cyclodextrins: studies for Indomethacin, Furosemide and Naproxen. J Incl Phenom Macrocycl Chem 56:29–32.
21. Yang W, de Villiers MM. 2004. Aqueous solubilization of furosemide by supramolecular complexation with 4-sulphonic calix[n]arenes. J Pharm Pharmacol 56:703–708.
22. Zvonar A, Berginc K, Kristl A, Gašperlin M. 2010. Microencapsulation of self-microemulsifying system: Improving solubility and permeability of furosemide. Int J Pharm 388:151–158.
23. Latere Dwan'lsa JP, Rouxhet L, Brewster ME, Préat V, Ariën A. 2008. Spontaneously self-assembled micelles from poly(ethylene glycol)-*b*-poly(ε-caprolactone-*co*-trimethylene carbonate) for drug solubilization. Pharmazie 63:235–240.
24. Shaji J, Jadhav D. 2010. Newer approaches to self emulsifying drug delivery system. Int J Pharm Pharm Sci 2:37–42.
25. Otsuka M, Onoe M, Matsuda M. 1993. Hygroscopic stability and dissolution properties of spray-dried solid dispersions of furosemide with eudragit. J Pharm Sci 82:32–38
26. Brittain HG. 2010. Cocrystal systems of pharmaceutical interest: 2007-2008. Profiles Drug Substances, Excipients Related Methodology 35:373–390.
27. Vishweshwar P, McMahon JA, Bis JA, Zaworotko MJ. 2006. Pharmaceutical Co-Crystals. J Pharm Sci 95:499–516.
28. Friščić T, Jones W. 2010. Benefits of cocrystallisation in pharmaceutical materials science: an update. J Pharm Pharmacol 62:1547–1559.
29. Desiraju GR. 1995. Supramolecular synthons in crystal engineering–A new organic synthesis. Angew Chem, Int Ed Engl 34:2311–2327.
30. Desiraju GR. 2007. Crystal Engineering: A holistic view. Angew Chem, Int Ed 46: 8342–8356.
31. Bhogala BR, Nangia A. 2003. Cocrystals of 1,3,5-cyclohexanetricarboxylic acid with 4,4' bipyridine homologues: Acid–pyridine hydrogen bonding in neutral and ionic complexes. Cryst Growth Des 3:547–554.
32. Caira MR. 2007. Sulfa drugs as model cocrystal formers. Mol Pharmaceutics 4:310–316 .
33. Ishida T, In Y, Doi M, Inoue M, Yanagisawa I. 1989. Structural study of Histamine H_2–receptor antagonists. Five

3-[2-(diaminomethyleneamino)-4-thiazolylmethylthio] propionamidine and amide derivatives. Acta Crystallogr B 45:505–512.
34. Goud NR, Babu NJ, Nangia A. 2011. Sulfonamide–pyridine-N-oxide cocrystals. Cryst Growth Des 11:1930–1939.
35. Pellegata RL. 1990. Furosemide salts. Patent US 5182300.
36. Carda-Broch S, Esteve-Romero J, Garcia-Alvarez-Coque MC. 2000. Furosemide assay in pharmaceuticals by micellar liquid chromatography: Study of the stability of the drug. J Pharm Biomed Anal 23:803–817.
37. Trask AV. 2007. An overview of Pharmaceutical cocrystals as Intellectual property. Mol Pharmaceutics 4:301–309 .
38. Babu NJ, Nangia A. 2011. Solubility Advantage of Amorphous Drugs and Pharmaceutical Cocrystals. Cryst Growth Des 11: 2662–2679.
39. GRAS chemical list. Accessed at www.fda.gov/Food/FoodIngredientsPackaging/GenerallyRecognizedasSafeGRAS/GRASSubstancesSCOGSDatabase/default.htm .
40. Childs SL, Stahly GP, Park A. 2007. The salt-cocrystal continuum: the influence of crystal structure on ionization state. Mol Pharmaceutics 4:323–328 .
41. Vogt FG, Clawson JS, Strohmeier M, Edwards AJ, Pham TN, Watson SA. 2009. Solid state NMR analysis of organic cocrystals and complexes. Cryst Growth Des 9:921–937.
42. Stevens JS, Byard SJ, Schroeder SLM. 2010. Salt or co-crystal? Determination of protonation state by x-ray photoelectron spectroscopy (XPS). J Pharm Sci 99:4453–4457.
43. Shan N, Toda F, Jones W. 2002. Mechanochemistry and co-crystal formation: Effect of solvent on reaction kinetics. Chem Commun 20:2372–2373.
44. Beyers H, Malan SF, van der Watt JG, de Villiers MM. 2000. Structure-solubility relationship and thermal decomposition of furosemide. Drug Dev Ind Pharm 26:1077–1083.
45. Li ZJ, Abramov Y, Bordner J, Leonard J, Medek A, Trask AV. 2006. Solid-state acid-base interactions in complexes of heterocyclic bases with dicarboxylic acids: Crystallography, hydrogen bond analysis and ^{15}N NMR spectroscopy. J Am Chem Soc 128:8199–8210.
46. Bernstein J, Davis RE, Shimoni L, Chang NL. 1995. Patterns in hydrogen bonding: Functionality and graph set analysis in crystals. Angew Chem, Int Ed Engl 34:1555–1573.
47. Chieng N, Rades T, Aaltonen J. 2011. An overview of recent studies on the analysis of pharmaceutical polymorphs. J Pharm Biomed Anal 55:618–644.
48. Trask AV, Jones W. 2005. Crystal Engineering of organic cocrystals by the solid-state grinding approach. Top Curr Chem 254:41–70.
49. Schultheiss N, Newman A. 2009. Pharmaceutical cocrystals and their physicochemical properties. Cryst Growth Des 9:2950–2967.
50. Li J, Bourne SA, Caira MR. 2011. New polymorphs of isonicotinamide and nicotinamide. Chem Commun 47:1530–1532.
51. Thompson LJ, Voguri RS, Male L, Tremayne M. 2011. The crystal structures and melting point properties of isonicotinamide cocrystals with alkanediacids $HO_2C(CH_2)_{n-2}CO_2H$, $n = 7–9$. CrystEngComm 13:4188–4195.
52. Vishweshwar P, Nangia A, Lynch VM. 2003. Molecular complexes of homologous alkanedicarboxylic acids with isonicotinamide: X-ray crystal structures, hydrogen bond synthons and melting point alternation. Cryst Growth Des 3:783–790.
53. Cherukuvada S, Babu NJ, Nangia A. Nitrofurantoin-*p*-aminobenzoic acid cocrystal: Hydration stability and dissolution rate studies. J Pharm Sci 100:3233–3244.
54. Childs SL, Chyall LJ, Dunlap JT, Smolenskaya VN, Stahly BC, Stahly GP. 2004. Crystal engineering approach to forming cocrystals of amine hydrochlorides with organic acids. Molecular complexes of fluoxetine hydrochloride with benzoic, succinic and fumaric acids. J Am Chem Soc 126:13335–13342.
55. Fahr A, Liu X. 2007. Drug-delivery strategies for poorly water soluble drugs. Expert Opin Drug Deliv 4:403–416.
56. Cheney ML, Shan N, Healey ER, Hanna M, Wojtas L, Zaworotko MJ, Sasa V, Song S, Sanchez-Ramos JR. 2010. Effects of crystal form on solubility and pharmacokinetics: a crystal engineering case study of lamotrigine. Cryst Growth Des 10:394–405.
57. Good D, Rodríguez-Hornedo N. 2009. Solubility advantage of pharmaceutical cocrystals. Cryst Growth Des 9:2252–2264.
58. Bethune SJ, Huang N, Jayasankar A, Rodríguez-Hornedo N. 2009. Understanding and predicting the effect of cocrystal components and pH on cocrystal solubility. Cryst Growth Des 9:3976–3988.
59. Jayasankar A, Reddy LS, Bethune SJ, Rodríguez-Hornedo N. 2009. Role of cocrystal and solution chemistry on the formation and stability of cocrystals with different stoichiometry. Cryst Growth Des 9:889–897.
60. Guo K, Sadiq G, Seaton C, Davey R, Yin Q. 2010. Co-crystallization in the caffeine/maleic acid system: Lessons from phase equilibria. Cryst Growth Des 10:268–273.
61. Powder Cell, a program for structure visualization, powder pattern calculation and profile fitting. Accessed at www.ccp14.ac.uk/tutorial/powdercell.
62. Cambridge Crystallographic Data Center, Cambridge Structural Database, version 5.32, November 2010, August 2011 update Available at www.ccdc.cam.ac.uk/products/csd.
63. SAINT-Plus, version 6.45. 2003. Madison, WI: Bruker AXS Inc.
64. Sheldrick GM. 1997. SADABS, program for empirical absorption correction of area detector data. Göttingen, Germany: University of Göttingen.
65. Sheldrick GM. 1997. SHELXS-97 and SHELXL-97, Göttingen, Germany: University of Göttingen.
66. Spek AL. 2002. PLATON, a multipurpose crystallographic tool. Utrecht, The Netherlands: Utrecht University.
67. Barbour LJ. 1999. X-Seed, graphical interface to SHELX-97 and POV-Ray. Columbia, MO: University of Missouri–Columbia.
68. Higuchi T, Connors KA. 1965. Phase-solubility techniques. Adv Anal Chem Instrum 4:117–212.